J Radioanal Nucl Chem
DOI 10.1007/s10967-015-4522-6

# Improved gamma-spectroscopy of marine samples via low background small anode germanium well detector with cosmic veto suppression

S. M. Pike[1] · A. S. Adekola[2] · J. Colaresi[2] · G. Ilie[2] · W. F. Mueller[2] · K. M. Yocum[2] · K. O. Buesseler[1]

Received: 17 June 2015


**Abstract** The small anode germanium (SAGe) Well detector from Canberra Industries with a cosmic veto supression system was tested on marine particles and water samples. The cosmic-veto suppression system reduced the shielded background by an average of 35 % across the energy spectrum. The enhanced energy resolution and efficiency improved the ability to separate the major U-238 decay chain energies 92, 238 and 241 keV $\gamma$ rays as well as separate the Cs-134 peak at 604 keV from the 609 keV $\gamma$-ray line of Bi-214. The SAGe Well detector with cosmic-veto suppression system has shortened counting times and increased sample throughput.

✉ S. M. Pike
spike@whoi.edu

A. S. Adekola
aderemi.adekola@canberra.com

J. Colaresi
jim.colaresi@canberra.com

G. Ilie
gabriela.ilie@canberra.com

W. F. Mueller
wilhelm.mueller@canberra.com

K. M. Yocum
mike.yocum@canberra.com

K. O. Buesseler
kbuesseler@whoi.edu

1 Department of Marine Chemistry and Geochemistry, Woods Hole Oceanographic Institution, 266 Woods Hole Road, Woods Hole, MA 02543, USA

2 CANBERRA Industries, Inc., 800 Research Parkway, Meriden, CT 06450, USA

**Keywords** Gamma ray spectrometry · Germanium well detector · Cosmic veto · Fukushima · Marine

## Introduction

Gamma-spectroscopy has a wide range of applications in the area of marine sciences. Significant advantages are its non-destructive nature and multiple isotope lines obtained from a single spectrum. Well detectors in particular have a proven advantage of greater counting efficiency which aids considerably in measuring low activities commonly associated with marine and environmental samples. Specifically, increasing the well volume within the crystal allows for a greater sample size and greater sensitivity. Sensitivity is enhanced further by increasing the size of the crystal and lowering the background of the detector resulting in a lower minimum detection activity [1]. This paper is intended to demonstrate advancements in energy resolution, sensitivity and background reduction provided by a new generation of well gamma detector coupled with a cosmic veto suppression system through a series of comparative analysis using a traditional high purity germanium well (Traditional Well) detector. Both systems were used to measure a constructed marine sediment standard. The standard was spiked with isotopes commonly associated with marine samples and measurements were used to evaluate resolution characteristics of both detectors. Results from comparative analysis of two marine samples from the study of natural and Fukushima derived radionuclides found in sinking particles and sea water processed through a Cesium extraction resin were used to further evaluate the new detector design through real application in research.

Published online: 15 October 2015

## The measurement system

The system used to quantify the samples is known as a Small Anode Germanium (SAGe) Well detector. The SAGe Well detector is a new design low capacitance germanium sensor with a well-type geometry [2]. The detector is a *p*-type elongated semi-planar detector type with a re-entrant well in the front face. As with Traditional Well detectors, the active germanium surrounds the well and inserted sample, and provides significantly increased solid angle sensor coverage around the sample and very high efficiency to detect emitted $\gamma$ rays.

In traditional germanium well detector designs, the energy resolution of the detector is dependent on the diameter of the sample well [3]. For this reason, the diameter of the sample well is typically restricted to relatively small size (typically 10–16 mm), which limits the volume of sample that can be accommodated in the well. At Woods Hole Oceanographic Institution, it was determined that the increased sample volume was preferable, and has deployed several Traditional Well detectors with 28 mm diameter sample wells. This comes with the expected decrease in energy resolution due to the large well. The recently developed SAGe Well detector has an electrode configuration that eliminates the energy resolution sensitivity to well diameter. This effect is illustrated in Fig. 1, which displays the measured energy resolution as a function of energy for a traditional design well detector and a SAGe Well detector. Both detectors have the same 28 mm diameter re-entrant well and accommodate the same size samples. The energy resolution is significantly better for the SAGe Well detector compared to the Traditional Well detector. This is particularly true at low energy. The improved energy resolution has significant effect on the sensitivity by improving the peak-to-background ratio for individual peaks and in some cases resolving peaks that would otherwise be difficult to analyze. The improved energy resolution of the SAGe Well detector is demonstrated from the resolution measurements presented in Fig. 2.

To improve the sensitivity, the detector is operated in a 10 cm thick lead shield to reduce the environmental background. The lead shield includes inner liners of tin and copper to reduce the background from X-ray fluorescence induced in the lead by cosmic-ray interactions. While the shield significantly reduces the background from terrestrial $\gamma$-ray sources, cosmogenic background sources are more penetrating. The lead shield provides only a partial shielding to signal inducing cosmic radiation. Further background reduction is obtained by introducing a 50 cm $\times$ 50 cm area by 4 cm thick scintillating plastic (EJ-200 [3]) detector on the top of the shield to be used to veto incoming cosmic events. A photograph of the setup is presented in Fig. 3. The output of the veto detector is processed through a digital tube multi-channel analyzer (MCA) [4] to generate a logic signal that is used as a gate input to the MCA [5, 6] connected to the SAGe Well detector. Coincident events between the plastic and germanium detectors are rejected under the assumption that the event is due to a highly penetrating cosmic event.

The quality of the suppression is determined by computing the cosmic suppression factor (CSF) with the following equation:

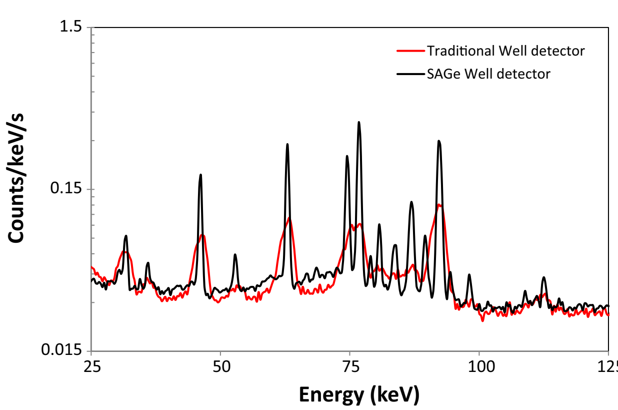


**Fig. 1** Measured energy spectra in the X-ray region for a radium sample measurement in the detector well. The same sample was measured in a Traditional Well detector and the SAGe Well detector. Both spectra are scaled to the same measurement time. The Traditional Well detector was operated in anti-coincidence with a veto detector which reduced the continuum background

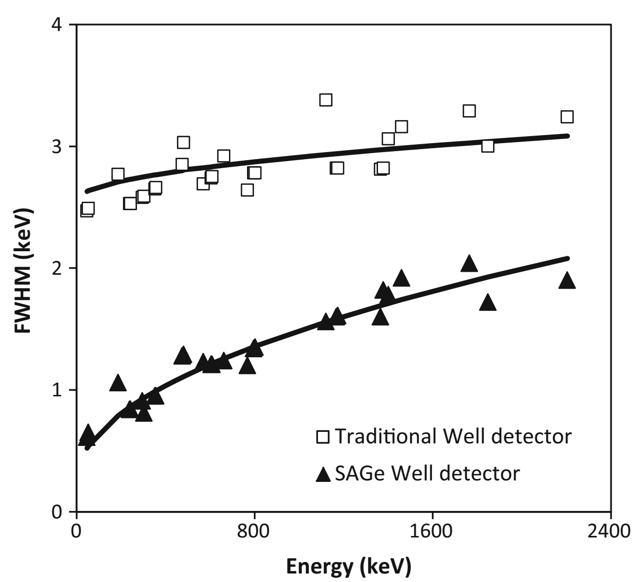


**Fig. 2** The measured full width at half maximum (FWHM) energy resolution for non-interfering $\gamma$ ray lines in a radium sample measured in the detector well. The results are for the same sample measured in the SAGe Well detector and a Traditional Well detector. Both spectra have comparable statistics in the peak areas. The *solid lines* represent fits to the data


**Fig. 3** Photograph of SAGe Well detector set up inside a 10 cm lead shield and a large area plastic detector used for cosmic-background suppression

$$\mathrm{CSF} = 1 - \frac{\sum_i C_i^{\mathrm{sup}}}{\sum_i C_i^{\mathrm{unsup}}}, \quad (1)$$

where $i$ is spectrum channel, $C_i^{\mathrm{sup}}$ is the number of counts in channel $i$ for the suppressed spectrum, and $C_i^{\mathrm{unsup}}$ is the number of counts in channel $i$ for the unsuppressed spectrum. This equation assumes that both spectra were acquired for the same live time and that the MCA gain settings are identical for both spectra. Using Eq. 1, the CSF was determined for the SAGe Well plus cosmic-veto setup, the results are presented in Fig. 4. These data show that the CSF is between about 20 and 30 %.

Critical to the proper operation of the cosmic-veto set up is that only cosmic induced events are rejected and that events from the sample are not rejected; for example, due to excessively high random coincidences. This possibility was checked by measuring a sample with and without cosmic veto suppression. Loss of counts in the peak area due to the cosmic veto shield were measured to be less than 2 %.

## Experimental

Since the earthquake and following tsunami off the east coast of Japan on March 11, 2011, this laboratory has participated in multiple research cruises investigating the largest accidental release of radiation to the marine environment from the damaged FNPP reactors [7, 8]. Between June 2011 and October 2014 hundreds of marine samples have been collected and analyzed via $\gamma$-ray spectroscopy. These samples came from near shore locations as well as transects across the Pacific Ocean, along the west coast of North America and beaches from Alaska to southern California to assess the dispersion of Cs-134 and Cs-137 in the western Pacific [9].

During this time CANBERRA Industries was embarking on the development of a new and innovative design of the SAGe Well detector and in 2012 invited the Radioanalytical Facility at Woods Hole Oceanographic Institution (WHOI) to be a beta-test site for this new detector. WHOI measured, analyzed and compared spectra from an absorber used to extract Cesium isotopes from sea water and sinking particles (SP) collected via sediment trap (McLane 7G-21) as part of the Fukushima research to quantify and validate the benefits the SAGe Well had over the existing Traditional Well. The results presented reflect benefits provided by the SAGe Well during analysis of marine samples collected as part of the investigation of radioactive release from the FNPP.

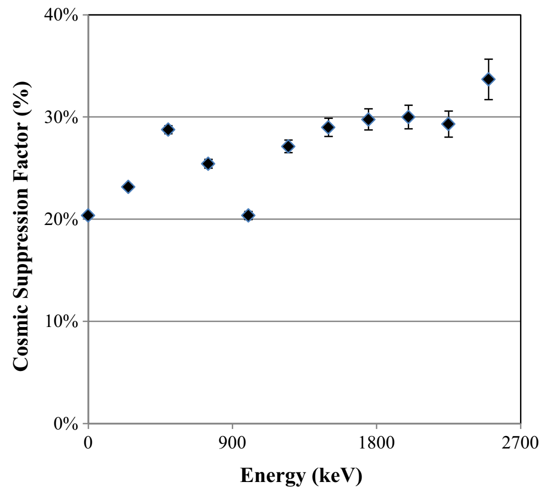


**Fig. 4** Cosmic suppression factor for the SAGe Well plus veto detector setup. The data were summed in 250 keV increments. The uncertainty *bars* represent the propagated statistical uncertainty of the measured spectra of SAGe Well detector

## Results and discussion

Initial evaluations of detector performance were made on a 10 mBq cm$^{-3}$ sediment standard (S1.31–35) with a counting density of 1.31 gm cm$^{-3}$ and a height of 35 mm. The $\gamma$-ray spectra for energy range of 40–250 keV presented in Fig. 5 shows a significant reduction in the

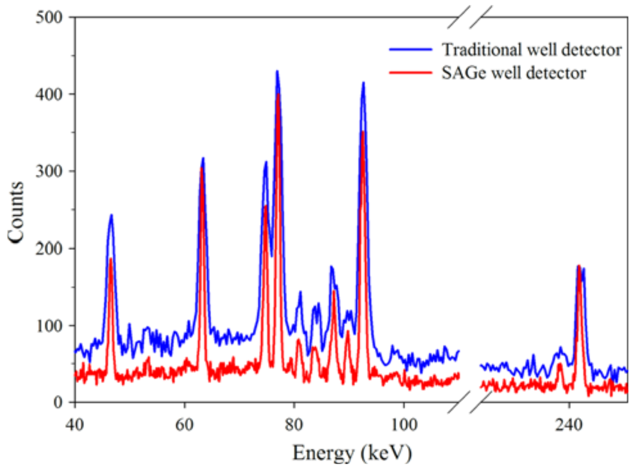


**Fig. 5** The measured low energy spectra for sediment standard S1.31–35 measured in both the SAGe Well and Traditional Well detectors. Both spectra are scaled to the same live time measurement of 7060 s and were operated in anti-coincidence mode with a veto detector

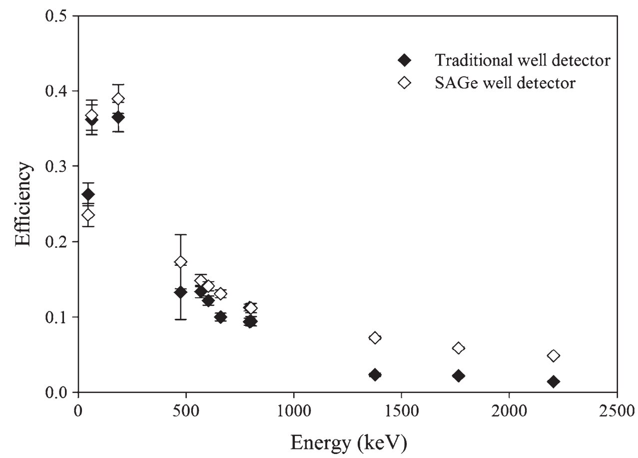


**Fig. 6** The measured efficiency of the SAGe Well detector (open) compared to the Traditional Well detector (filled) for the 10 mBq cm$^{-3}$ sediment standard (S1.31–35) with a counting density of 1.31 g cm$^{-3}$ and a fill height of 35 mm

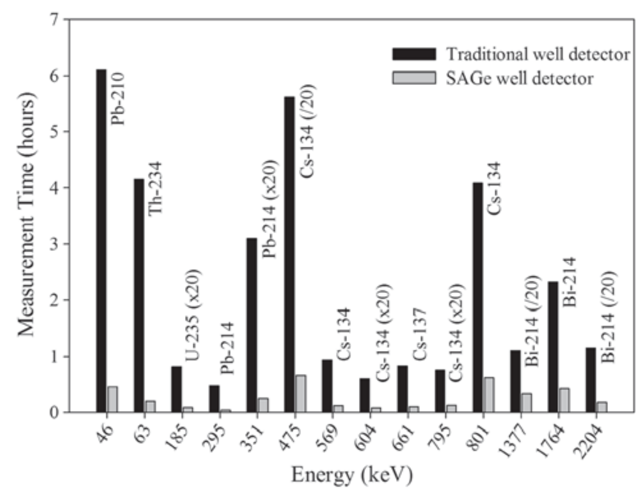


**Fig. 7** Time to measure 10 mBq cm$^{-3}$ at 5σ above background for the S1.31–35 standard with fill height of 35 mm. Note the measurement time for the 1377, 2204 and 475 keV lines were divided by 20 to make them fit into the spectrum. The measurement time of the 185, 351,604 and 795 keV lines were multiplied by 20 to make them visible in the spectrum

background of the SAGe Well. During this initial performance evaluation, the SAGe Well resolution was determined to be better by a factor of 4 at 45 keV (from 2.49 to 0.61 keV FWHM) compared to the Traditional Well and more than 35 % at the higher energies. SAGe Well detector demonstrated better resolution performance over Traditional Well detector as presented in Fig. 2 by separating the Th-234 $\gamma$-ray line at 92.5 keV from the 90 keV, the 74 and 76 keV X-ray lines and the 238 and 241 keV $\gamma$-ray lines of Pb-212 and Pb-214 in the spectrum.

The efficiency of a detector is geometry dependent and the SAGe Well has improved efficiency over the Traditional Well because of its' larger crystal volume. The SAGe Well has a diameter of 8.24 cm and a length of 6.36 cm, while the Traditional Well has a diameter of 6.48 cm and length of 6.44 cm. The peak efficiency for both detectors was determined at key energy lines in Cs-137, Cs-134 and U-238 nuclides and is shown in Fig. 6. The combination of better energy resolution and efficiency results in an improved overall performance which is evident through a comparison of measurement time of our standard sample. Calculations were made for the time to achieve a measurement of a given radionuclide to a five standard deviation confidence level using the following formula:

$$t[\mathrm{h}] = \frac{5(2\delta E)\dot{B}}{3600A^2\varepsilon^2Y^2} \quad (2)$$

where $\delta E$ is the full-width at half-maximum (FWHM) energy resolution, $\dot{B}$ is the background rate in count/sec/keV, $A$ is the activity in Bq, $\varepsilon$ is the efficiency, and $Y$ is the per decay yield of the $\gamma$-ray associated with the particular radionuclide of interest. The assumption of this formula is that the region of interest (ROI) around each peak is set to 2 times the FWHM resolution of the peak. This formula does not account for true and random coincidence summing effects. Measurement time for 10 mBq of key radionuclides of interest are presented in Fig. 7. In comparing the results, one can observe that the SAGe Well detector has an significant improvement in performance over Traditional Well detector. This is due to the combination of background suppression from the cosmic-ray veto, better energy resolution and greater efficiency.

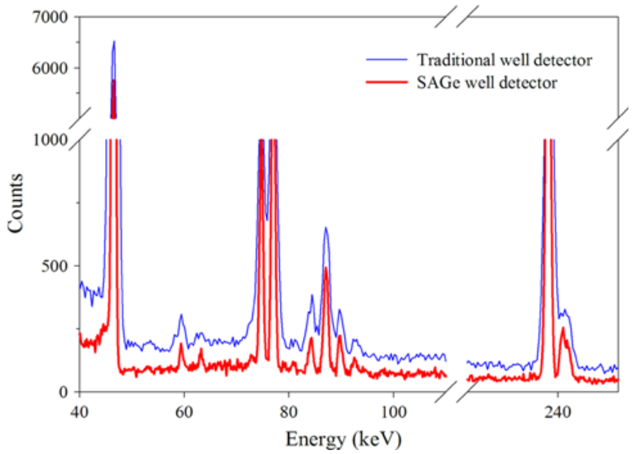


**Fig. 8** The measured low energy spectra for sinking particles collected by sediment traps in December 2013. The sample was measured by the SAGe Well detector and the Traditional Well detector. Both spectra are scaled to the same live time measurement 0f 80,700 s and were operated in anti-coincidence mode with a veto detector

The improved characteristics of the SAGe Well were further tested through the comparative analysis of two types of marine samples. First examined were sinking particles from a sediment trap collected over an eighteen day period from a depth of 1000 m in December of 2013. The trap was part of a time series investigation of Fukushima derived contaminants and is located 60 nautical miles south of FNPP at station F1. Particles were sieved through a 1 mm plastic mesh and the filtrate was dried and pulverized [10]. The sample was then transferred to a polycarbonate counting vial, weighed and the height measured for efficiency determination.

Figure 8 shows the low energy spectra of the sample measured by both detectors and demonstrated is the reduction in the background and improved resolution of the SAGe Well detector. Some of the short lived U-238 lower energy daughters seen in the sediment standard have decayed away but the longer lived lead isotopes at 238 and 242 keV have been clearly separated by the SAGe Well. In Table 1, spectra data for key energy lines are presented and missing in these results is data where the Traditional Well was unable to resolve two close energy peaks. The ratio of total counts of Cs-137 at 661 keV and two Cs-134 peaks at 604 and 795 keV shows an increase in sensitivity for the SAGe Well by 20–40 %.

A similar comparison was made on a twenty liter sea water sample collected approximately 10 km south of FNPP in October 2014 as part of the continued monitoring of release from the reactor. The sample was passed through KNiFC-PAN, an absorber specific for the extraction of Cesium, transferred to a polycarbonate counting vial, dried and $\gamma$ counted using equal live time presets [11–13]. Although the absorber is designed to preferentially remove Cesium, in some samples a significant amount of Pb-214 and its' decay product Bi-214 is removed during the extraction process and seen in the $\gamma$-ray spectrum. As of now this phenomenon does not correlate to the type of sample undergoing extraction such as ground water, coastal or open ocean sea water. Spectra data for three Cesium energies of interest are given in Table 2 shows an increase in sensitivity of between 10 and 50 % for these isotopes provided by the SAGe Well.

## Conclusions

The design of the SAGe Well detector has produced higher energy resolution and efficiencies. Through the integration of a cosmic-veto suppression system a 40 % reduction in

**Table 1** Spectra data for sinking particles collected by sediment traps in December 2013

| Detector | Sinking particles | | | FWHM (keV) | Area (counts) | Error (%) |
|---|---|---|---|---|---|---|
| | Left marker (keV) | Right marker (keV) | Centroid (keV) | | | |
| SAGe well | 44.1 | 47.8 | 46.4 | 0.603 | 26,279 | 0.7 |
| | 236.9 | 239.6 | 238.4 | 0.907 | 11,845 | 1.0 |
| | 239.8 | 242.9 | 241.7 | 0.913 | 758 | 5.9 |
| | 349.8 | 353.1 | 351.6 | 1.005 | 2964 | 2.3 |
| | 602.2 | 606.7 | 604.3 | 1.270 | 1598 | 3.3 |
| | 658.8 | 663.6 | 661.2 | 1.293 | 9074 | 1.1 |
| | 793.0 | 797.3 | 795.3 | 1.278 | 1015 | 3.6 |
| Trad. well | 44.0 | 48.9 | 46.4 | 1.480 | 29,758 | 0.6 |
| | 348.6 | 355.8 | 352 | 1.615 | 2351 | 2.9 |
| | 601.3 | 606.9 | 604.6 | 1.802 | 1204 | 3.3 |
| | 656.8 | 666 | 661.5 | 1.736 | 6432 | 1.4 |

**Table 2** Spectra data for sea water collected off FNNP in October 2014

| Detector | Sea water | | | FWHM (keV) | Area (counts) | Error (%) |
|---|---|---|---|---|---|---|
| | Left marker (keV) | Right marker (keV) | Centroid (keV) | | | |
| SAGe well | 601.9 | 606.7 | 604.4 | 1.290 | 359 | 7.8 |
| | 659.3 | 663.6 | 661.3 | 1.348 | 3126 | 2.2 |
| | 793.8 | 797.2 | 795.4 | 0.557 | 226 | 14.3 |
| Trad. well | 601.3 | Unresolved | 604.6 | 1.941 | 224 | 11.7 |
| | 657.5 | 665.7 | 661.5 | 1.680 | 2134 | 2.9 |
| | 792.9 | 798.5 | 795.8 | 1.890 | 209 | 10.9 |

background and lower MDA is achieved. These combined improvements have resulted in shortened counting times and allowed for increased sample throughput; making timely analysis of large numbers of samples more feasible. Samples of marine particles and sediment do not undergo isolation or purification steps prior to gamma counting. The increase in energy resolution has allowed for the separation of many interfering $\gamma$ lines produced from natural and artificial isotopes and their multiple decay series present in a sample. Results from these analyses have been used in evaluation of trapping efficiencies as well as understanding marine processes affecting the vertical transport and eventual fate of contaminant radionuclides. Results from sea water analysis have been integrated into the larger study of mapping and transport of continued releases of Cesium from the Fukushima NPP.

**Acknowledgments** This research was made possible by grants from the Gordon and Betty Moore Foundation, the Deerbrook Foundation and Woods Hole Oceanographic Institution. We would like to thank the Captain and crew of the R/V *Tunsei Maru* and R/V *Shinsei Maru* for all their efforts towards the successful collection of marine samples presented in this paper.

## References

1. Andrews JE, Hartin C, Buesseler KO (2008) Beryllium-7 analyses in seawater by low background gamma spectroscopy. J Radioanal Nucl Chem 277(1):253–259
2. Adekola AS, Colaresi J, Douwen J, Mueller WF, Yocum KM (2014) Performance of a small anode germanium well detector. Nucl Instr Method A. doi:10.1016/j.nima.2014.12.034
3. Germanium Well Detector (WELL). http://www.canberra.com/products/detectors/pdf/Germanium-Well-C39793.pdf. Accessed 13 Mar 2015
4. EJ-200. http://www.eljentechnology.com/index.php/products/plastic-scintillators/48-ej-200. Accessed 5 Mar 2015
5. Osprey—Universal Digital MCA tube base for scintillation spectrometry. http://www.canberra.com/products/radiochemistry_lab/pdf/Osprey-SS-C40303.pdf. Accessed 13 Mar 2015
6. Lynx digital signal analyzer. http://www.canberra.com/products/radiochemistry_lab/pdf/Lynx-SS-C38658.pdf. Accessed 13 Mar 2015
7. Buesseler KO, Aoyama M, Fukasawa M (2011) Impacts of the Fukushima nuclear power plants on marine radioactivity. Environ Sci Technol 45:9931–9935
8. Buesseler KO, Jayne SR, Fisher NS, Rypina II, Baumann H, Baumann Z, Breier CF, Douglass EM, George J, Macdonald AM, Miyamoto H, Nishikawa J, Pike SM, Yoshida S (2012) Fukushima-derived radionuclides in the ocean and biota off Japan. PNAS. doi:10.1073/pnas.1120794109
9. Rypina II, Jayne SR, Yoshida S, Macdonald AM, Douglass E, Buesseler KO (2013) Short-term dispersal of Fukushima-derived radionuclides off Japan: modeling efforts and model-data intercomparison. Biogeosci Discuss 10:1517–1550. doi:10.5194/bgd-10-1517-2013
10. Honda MC (2013) Fukushima-derived radiocesium in western North Pacific sediment traps. Biogeosci Discuss 10:2455–2477. doi:10.5194/bgd-10-2455-2013
11. Sebesta F (1997) Composite sorbents of inorganic ion-exchangersand polyacrylonitrile binding matrix. J Radioanal Nucl Chem 288(2):603–611
12. Pike SM, Buesseler KO, Breier CF, Dulaiova H, Stastna K, Sebesta F (2013) Extraction of cesium in seawater off Japan using AMP-PAN resin and quantification via gamma spectroscopy and inductively coupled mass spectrometry. J Radioanal Nucl Chem 296:369–374. doi:10.1007/s10967-012-2014-5
13. Kamenık J, Dulaiova H, Sebesta F, Stastna K (2013) Fast concentration of dissolved forms of cesium radioisotopes from large seawater samples. J Radioanal Nucl Chem. doi:10.1007/s10967-012-2007-4